

Dedicated to Acad. Prof. Dr. Margareta Giurgea with the occasion of her 90-th anniversary

## LASER INDUCED SOLITON WAVEGUIDES IN LITHIUM NIOBATE CRYSTALS FOR GUIDING FEMTOSECOND LIGHT PULSES

A. Petris, A. Bosco<sup>a</sup>, V. I. Vlad<sup>\*</sup>, E. Fazio<sup>a</sup>, M. Bertolotti<sup>a</sup>

Inst. Atom. Phys, NILPRP-Romanian Center of Excellence in Photonics, Bucharest, Romania

<sup>a</sup>Univ. "La Sapienza" e INFN, Dipartimento di Energetica, Via Scarpa 16, I-00161 Roma, Italy

We show that efficient waveguides can be written by bright spatial solitons in lithium niobate photorefractive crystals by c.w. and pulsed laser beams. Using high repetition rate femtosecond laser pulses, an efficient formation of soliton waveguides is possible, after accumulating a large number of pulses, because the photo-excited carrier relaxation time is much longer than the pulse period. These results open the possibility of optimum waveguiding the femtosecond pulsed laser beams, the soliton waveguides creating a graded refractive index profile matched to the spatial beam profile. Our experiments show also very low pulse dispersion in these waveguides.

(Received July 4, 2005; accepted July 21, 2005)

*Keywords:* Optical waveguides, Spatial solitons, Photo-refractive crystals

### 1. Introduction

Lithium niobate ( $\text{LiNbO}_3$  - LNB) is a widely used material for optoelectronic applications. Among all the effects that this material is offering, we shall focus our attention on the electro-optic one, which made LNB exhibit photorefractive properties. Photorefractive nonlinearities in LNB are based either on the generation of a local photovoltaic electric field [1], or the generation of bound carrier populations, that can produce a screening of an uniform externally applied bias [2], or on a combination of the two [2,3]. Following these possibilities, analytical predictions have been made for obtaining spatial solitons, either bright or dark [3,4,5]. Experimentally dark solitons have been observed [6,7,8] without any external bias, in both open and closed circuit configurations [9]. Transition from defocusing to focusing behavior of photovoltaic nonlinearities have been predicted and experimentally observed in the open-circuit configuration [10], opening the possibility of bright photovoltaic soliton generation in LNB. Screening-photovoltaic bright solitons were indeed observed and experimentally characterized [11] using a CW laser beam in the green. In such a case, a strong bias was applied to increase the screening field with respect to the photovoltaic one. It must be pointed out here that all the experimental testing for photorefractive soliton generation have been performed either with CW laser light or with relatively long pulses [12] (100 ps).

In this paper, we show that bright photorefractive soliton waveguides (SWGs) can be written in LNB photorefractive crystals by c.w. and pulsed laser beams. Using high repetition rate femtosecond laser pulses, an efficient formation of SWGs is possible, after accumulating a large number of pulses, because the photo-excited carrier relaxation time [10] is much longer than the pulse period. This opens the possibility of optimum waveguiding the femtosecond laser beams, the corresponding SWGs showing a graded refractive index profile matched to the beam profile. Our experiments reveal also very low pulse dispersion in these waveguides.

---

\* Corresponding author: vlad@ifin.nipne.ro

## 2. Bright soliton waveguide formation in LNB with c.w. laser beams at 514 nm for guiding femtosecond laser pulses

We have used the experimental set-up shown in Fig. 1 for generation of SWGs in the intrinsic LNB crystals and the propagation of femtosecond laser pulses through these waveguides.

In a first experiment, the laser beam from a c.w. Argon ion laser ( $\lambda = 514$  nm), linearly polarized, with a Gaussian transversal intensity distribution, was split into two beams for signal and background. The signal beam is focused to about  $9 \mu\text{m}$  on the input face of the crystal of 5 mm thickness ( $\sim 5$  diffraction lengths). This beam propagated along the z-direction, orthogonally to the optical axis (y-direction). A bias voltage is applied on the LNB crystal along the optical axis. The background beam, which is mutually incoherent to the signal beam, is expanded and sent along the x-direction in the crystal. The crystal is immersed in a cell with insulating oil, placed on a stage that allows the fine adjustment of the crystal position for optimum coupling of the probe beam to the different SWGs induced in the crystal. An imaging system is used to visualize the transversal shape of the signal beam at the input and output planes of LNB crystal.

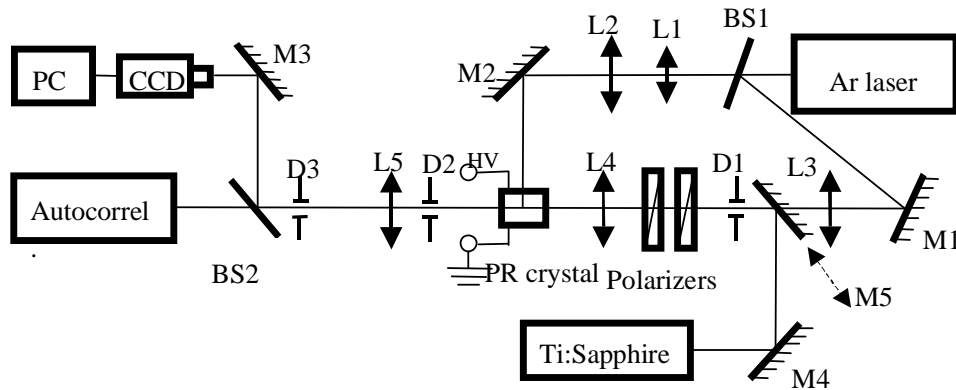


Fig. 1. Experimental set-up for generation soliton waveguides with a c.w. (Argon ion laser) and to study the propagation of femtosecond laser pulses through such waveguides.

The temporal evolution of the beam shape at the output plane is shown in the Fig. 2a, for a static bias  $E_0 = 35$  kV/cm and a ratio  $r \sim 3300$  between the intensity of the signal beam ( $I_s = 8.6$  W/cm<sup>2</sup>, signal power  $10 \mu\text{W}$ ) and of the background beam ( $I_b = 2.6$  mW/cm<sup>2</sup>). The full procedure for SWGs writing is described in [19, 20].

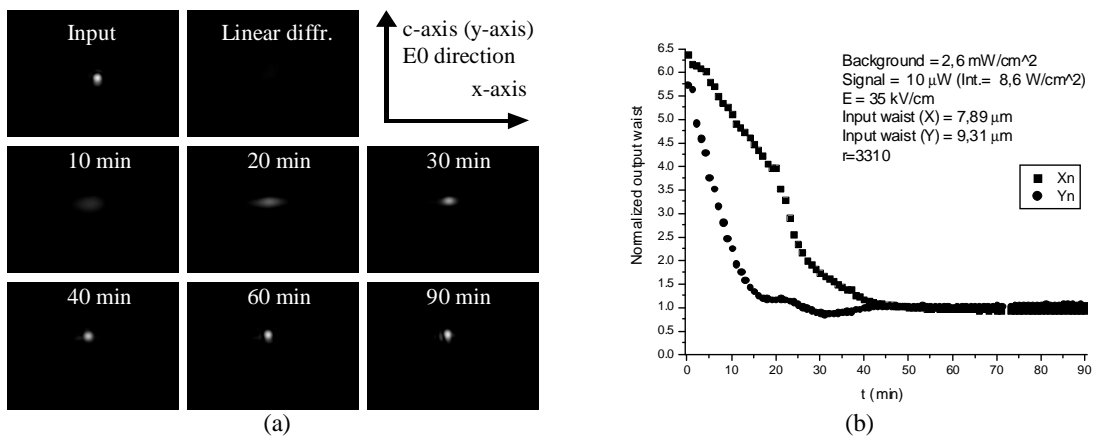


Fig. 2. The temporal evolution of the transversal shape of the signal beam at the output of the crystal (a) and of the normalized output beam widths along the x and y-axis (b).

The soliton waveguide becomes cylindrical with circular sections at  $E_0 = 35$  kV/cm and with a c.w. exposure for about 30 min. (Fig. 2b). After this time, no noticeable changes in beam waists along the two directions appear. Different guiding properties can be obtained depending on the duration of the SWG writing. If cutting the voltage on the crystal when the confinement is reached on y-direction, the soliton channel has guiding properties mainly on this direction.

The temporal stability of the induced SWGs was checked for times up to 1 month by monitoring their guiding properties when coupling to waveguide, for short times, the light with the same wavelength as used for writing. No effective change of the output profile of the beam transmitted through waveguide was observed.

The soliton waveguides induced in the LNB crystal were tested by guiding 75 fs pulses generated by a mode-locked Ti:Sapphire laser. Several waveguides induced for different recording times in the same LNB crystal have been investigated: WG 1 – 15 min recording time, WG2 and WG 3 – 30 min, WG 4 – 60 min, WG 5 and WG 6 – 90 min. The beam with 35 mW average power, injected in the waveguides, was vertically polarized. We compared the signal beam shape at the input with the beam shape at the output, within or outside the six different soliton waveguides. The results are shown in Fig. 3.

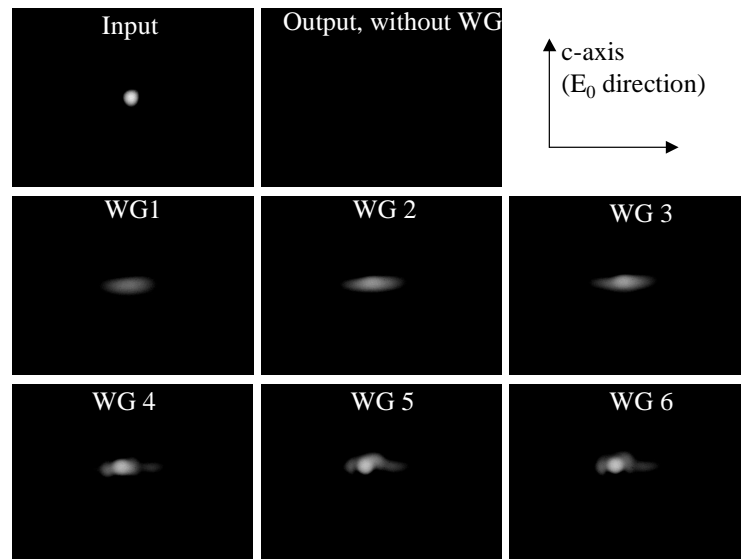


Fig. 3. Guiding femtosecond laser beams through SWGs created by a low power (10  $\mu$ W) c.w. argon laser.

In order to check the guiding properties of the induced soliton waveguides, we have acquired the laser beam images in the input and the output planes of the crystal and we have also visually observed the beam profile along its propagation through the crystal. In Fig. 4, we have shown the corresponding beam profiles fitted with Gaussian curves (the input beam and output beam, passing through the crystal, outside waveguides) and hyperbolic secant curve (the output beam passing through a soliton waveguide) respectively. We can assert that the beam profiles conserve their widths over  $\sim 5$  diffraction lengths of propagation.

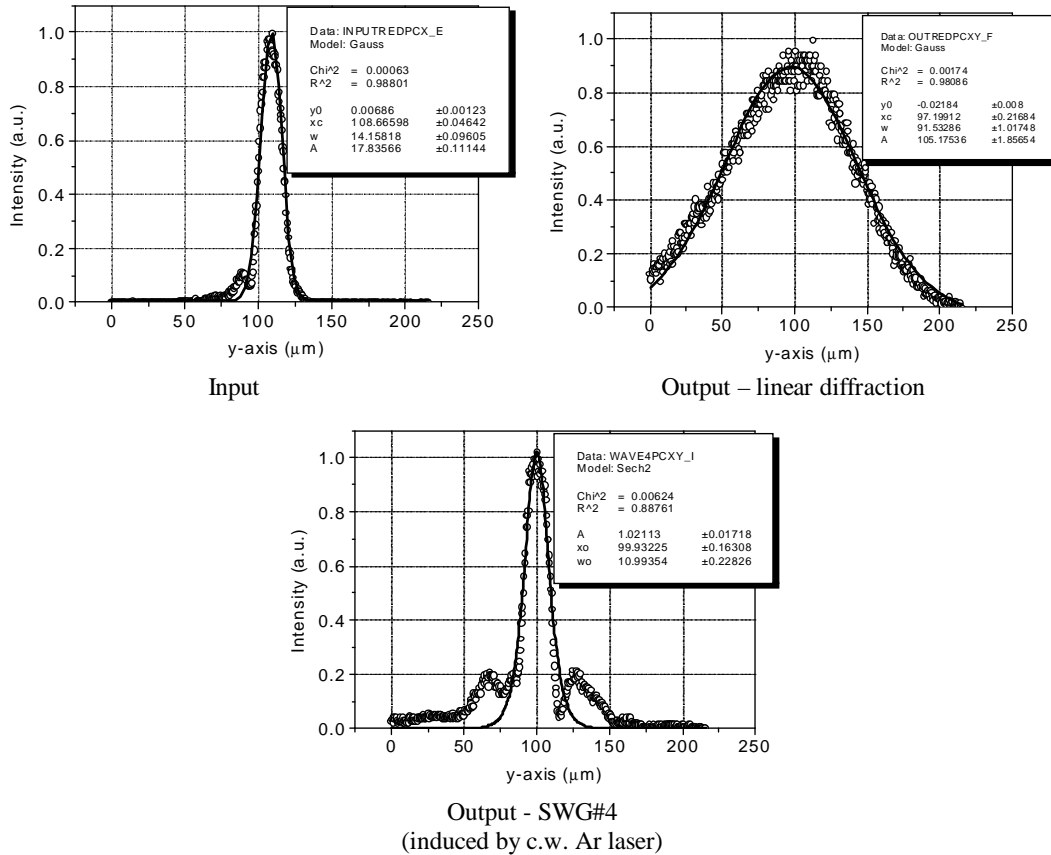


Fig. 4. The beam profiles in the input and the output planes of LNB crystal in the case of free propagation through the crystal and the output of SWGs induced by c.w. Ar laser.

We measured the change of the pulse duration produced by the soliton waveguides. For these measurements we used an autocorellator (Femtoscope) coupled to a PC, in the intensimetric (background free) mode of operation. The temporal profile of the fs pulses was very well fitted by a  $\text{sech}^2$  curve (Fig. 5). In all measurements the crystal remained immersed in the cell with insulating oil. The pulse durations, for these different paths, were obtained by averaging 20 different measurements done with the autocorellator. In each measurement, 150 acquisition sequences (each of them of 40 scans) were averaged by the Femtoscope.

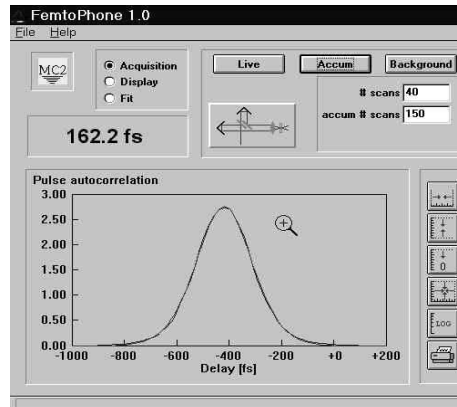


Fig. 5. The pulse duration at SWG output measured with an autocorrelator, in the intensimetric (background free) mode of operation. The temporal profile of femtosecond pulses was very well fitted by a sech<sup>2</sup> curve.

In Table 1, the output pulse durations for: a) fs-beam passing through the cell with oil (near to the crystal), b) fs-beam passing through the crystal in a region where is not induced a waveguide and c) fs-beam passing through the six different waveguides induced in the crystal (previously mentioned) are compared.

Table 1.

Material	Oil	Crystal	WG1 15 min	WG2 30 min	WG3 30 min	WG4 60 min	WG5 90 min	WG6 90 min
Average pulse duration (fs)	112.4	164.1	164.9	166.0	165.8	169.4	168.2	169.2
Error (fs)	1.2	2.1	1.8	2.4	1.9	2.5	1.7	1.5

In comparison with the large change of the pulse duration induced by the cell with oil and the crystal, only a very small increasing of the pulse duration is produced by the soliton waveguides ( $\sim 10$  fs/mm).

### 3. SWG formation in LNB with femtosecond pulsed laser beams with wavelength of 800 nm for guiding femtosecond laser pulses

The experimental set-up is shown in Fig. 6. A nominally pure LNB crystal, 5 mm long, was electrically biased at 35 kV/cm along its optical-axis direction ([001] crystallographic direction). A light beam from a Ti:Sapphire laser, at wavelength 800 nm, was focused down to about 9  $\mu\text{m}$  (HWHM) on the input (100) face of the crystal. This beam consists of pulses of 75 fs at the input face, at the repetition rate of 78 MHz and has an average power of 16 mW. The linear dispersion of the pulses inside the LNB crystal was 9.9 fs/mm; nonlinear dispersion was negligible. Experimental measurements were performed with a uniform background illumination: such an illumination was obtained by using a c.w. Argon-ion laser beam, at 514 nm, expanded and sent to the (010) crystal face. At the end, the output crystal face was imaged on the CCD sensor of a computer interfaced camera.

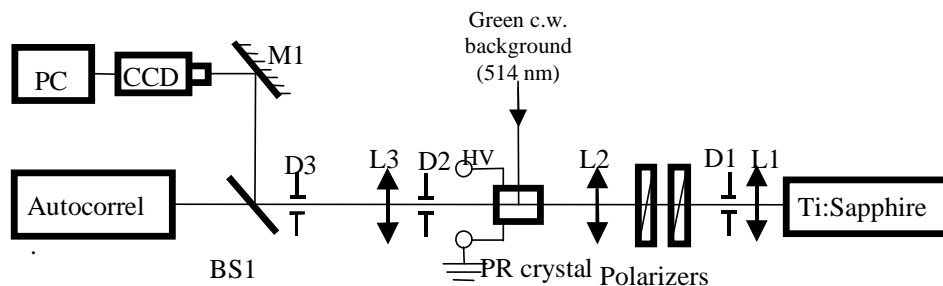


Fig. 6. Experimental set-up for generation soliton waveguides with a femtosecond pulsed laser beam with wavelength of 800 nm and for study the propagation of femtosecond laser pulses through induced waveguides.

The dynamics of the Ti:Sapphire laser beam propagating inside the LNB crystal, with the background illumination, is shown in Fig. 7, where the beam profile at the input face is shown for comparison. The linear diffraction inside the crystal is evident at the initial experimental time (0 min), for which both the bias and the beam were turned on. The background beam was set in order to give an uniform illumination of  $\sim 10$  mW/cm<sup>2</sup>. In such a case, the self-focusing was very efficient since the first minutes, firstly along the vertical direction, which corresponds to the optical axis of

the crystal. This process was already observed in c.w. regime [11], where the beam confinement along this axis was faster than along the other one. As shown in Fig. 7, the bright soliton size ( $20 \pm 1 \mu\text{m}$ , FWHM) along the vertical axis was reached after 8 min, while along the horizontal axis, it was slower, reaching the same size after about 11 min. As previously reported [20], solitons with circular sections (single-mode fibre type) are obtained also in this experiment with LNB; however due to high light intensity ( $1.1 \text{ GW}/\text{cm}^2$ ) and the high bias field applied ( $35 \text{ kV}/\text{cm}$ ), a bending of the beam was observed, as high as  $40\text{-}50 \mu\text{m}$ , which slightly distorts the beam.

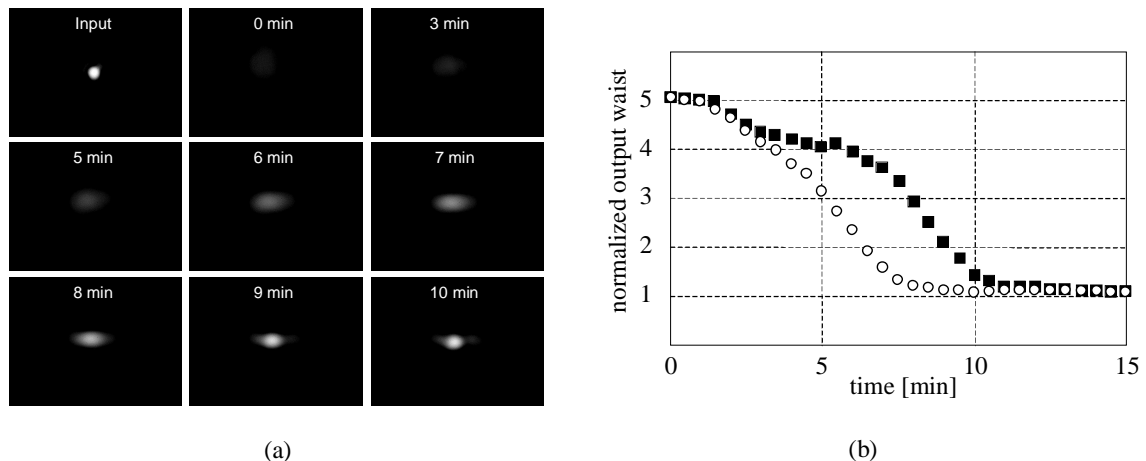


Fig. 7. (a) The dynamics of the soliton waveguides induced with a femtosecond pulsed laser beam (800 nm) with c.w. green background illumination (514 nm); (b) The temporal evolution of the bright soliton formation (output waist normalized to the input one) along the y-axis (optical axis of the crystal) (open circles) and x-axis (closed squares) of the beam profile.

An explanation of the soliton formation in LNB crystal, which shows low sensitivity in the red spectral domain, can be given as follows. When the short-pulse beam at 800 nm is injected in the sample, two main absorption processes occur, direct transitions from shallow traps [1] and two-photon-absorption [13,14,15,16] (TPA). Both these processes, as previously reported, can occur in pure LNB, being completely independent from the doping level or purity of the crystal. TPA can even overpass the linear absorption for high intensities: in our case, the linear absorption was as high as  $0.06 \text{ cm}^{-1}$ , while the TPA, at  $1 \text{ GW}/\text{cm}^2$ , was  $0.25 \text{ cm}^{-1}$ , i.e. 4 times larger.

The laser beam absorption at 800 nm (without green background illumination) produces transitions, which lead to a free carrier population. Free-carriers are then mobilized by the photovoltaic field (PVF), which is much stronger in the center of the Gaussian beam than at the boundary. In nominally undoped crystals, such carriers have large average-free-paths before recombining and give rise to a weak current flow. The bound ionized species, occurring inside the beam, generate a screening field (SF) for the external and for the photovoltaic fields. This non-uniform SF starts to produce the self-focusing of the laser beam. However, it is not enough to balance PVF (typically, of the order of  $10 \text{ kV}/\text{cm}$ ), which remains dominant in the core of the laser beam. PVF leads to a negative variation of refractive index, which may support the formation of a dark soliton. This dark soliton is not stable because its bright sides are bell-shaped [17] and force it to split in other two dark solitons.

When an uniform green background shines also the LNB crystal (together with the red femtosecond pulsed laser), absorption from deep levels occurs all around and yields an uniform distribution of ionized traps. These traps strongly reduce the average-free-path of the carriers excited by the red laser beam (800 nm) and they recombine with the bound ionized species in a volume approximately limited by the beam boundary. Consequently, SF is now well localized inside the red beam and may overpass PVF. In this case, SF induces light self-trapping and possible formation of bright solitons.

In our case, the green background cannot favor the absorption in (infra-)red (800 nm), which was observed [12,18] in doped LNB only, with green light intensities much higher than those used here (few mW/cm<sup>2</sup>).

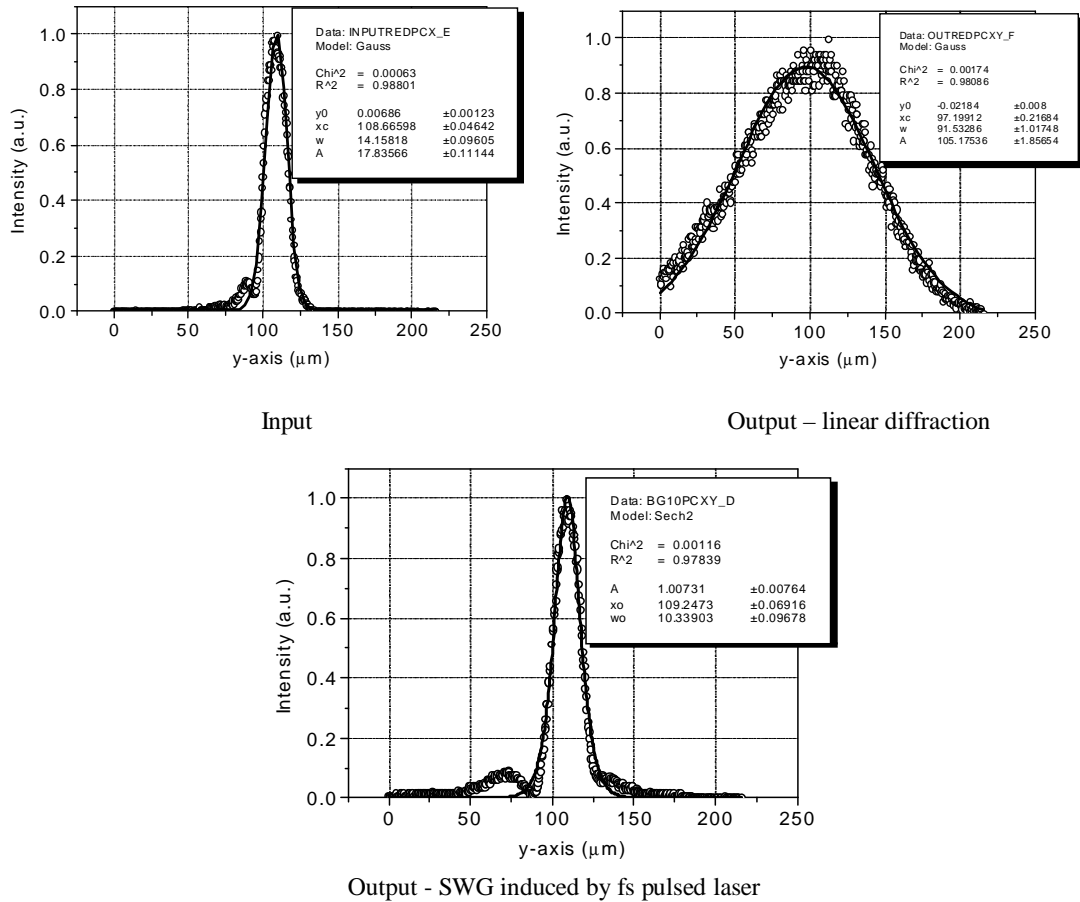


Fig. 8. The beam profiles in the input and the output planes of LNB crystal in the case of free propagation through the crystal and for SWGs induced by femto-laser with a c.w. green Background.

When propagating femtosecond laser pulses through self-written SWGs (Fig. 7 and 8), the pulse evolution is similar to that observed in c.w. produced SWGs (see Fig. 4 and Table 1). Moreover, one can observe a smaller perturbation of the beam shape at the output of the SWG in LNB crystal, which can be explained by the wavelength matching in this case.

#### 4. Conclusions

Solitons provide an easy and fast way for writing waveguides which are matched to the laser beam profiles. SWGs in LNB were stored for long times with efficient guiding properties and can be also erased on demand. Bright spatial solitons were created in LNB crystals with low power c.w. green lasers. These SWGs show low dispersion for ultrashort laser pulse propagation and can be used in efficient reconfigurable optical interconnections.

Using high repetition rate femtosecond laser pulses with the wavelength of 800 nm, an efficient formation of bright soliton waveguides was shown in undoped LNB (which is low sensitive at this wavelength), when using an additional uniform background illumination of the crystal at the

wavelength of 514 nm. The soliton formation was observed after accumulating a large number of pulses, because the photo-excited carrier relaxation time was much longer than the pulse period. The background illumination decreases the average-free-path of free carriers, making the screening effect to dominate over the photovoltaic one. These results open the possibility of optimum waveguiding the femtosecond pulsed laser beams, the soliton waveguides creating a graded refractive index profile matched to the spatial beam profile.

### Acknowledgements

This work has been supported by the project #36 of the Bilateral Collaboration Agreement in R&D between Italy and Romania and CNCSIS Grant #1141.

### References

- [1] A. M. Glass, D. von der Linde, T.J. Negran, *Appl. Phys. Lett.* **25**, 233 (1974).
- [2] A. M. Glass, *Opt. Engineering* **17**, 11 (1978).
- [3] L. Keqing, Z. Yanpeng, T. Tiantong, H. Xun, *J. Opt. A: Pure Appl. Opt.* **3**, 262 (2001).
- [4] G. C. Valley, M. Segev, B. Crosignani, A. Yariv, M. M. Fejer, M. C. Bashaw, *Phys. Rev. A* **50**, R4457 (1994).
- [5] H. Chun-Feng, L. Bin, S. Xiu-Dong, J. Yong-Yuan, X. Ke-Bin, *Chinese Physics* **10**, 310 (2001).
- [6] M.Taya, M. C. Bashaw, M. M. Fejer, M. Segev, G. C. Valley, *Phys. Rev. A* **52**, 3095 (1995).
- [7] Z. Chen, M. Segev, D. W. Wilson, R. Muller, P. D. Maker, *Phys. Rev. Lett.* **78**, 2948 (1997).
- [8] G. Couton, H. Maillotte, R. Giust, M. Chauvet, *Electr. Lett.* **39**, 286 (2003).
- [9] M. Chauvet, *J. Opt. Soc. Am. B* **20**, 2515 (2003).
- [10] C. Anastassiou, M. Shih, M. Mitchell, Z. Chen, M. Segev, *Opt. Lett.* **23**, 924 (1998).
- [11] E. Fazio, F. Renzi, R. Rinaldi, M. Bertolotti, M. Chauvet, W. Ramadan, A. Petris, V. I. Vlad, *Appl. Phys. Lett.* **85**, 2193 (2004).
- [12] N. Fressengeas, D. Wolfensberger, J. Maufoy, G. Kugel, *J. Appl. Phys.* **85**, 2062 (1999).
- [13] D. von der Linde, A. M. Glass, K. F. Rodgers, *Appl. Phys. Lett.* **25**, 155 (1974).
- [14] D. von der Linde, A.M. Glass, K. F. Rodgers, *J. Appl. Phys.* **47**, 217 (1976).
- [15] H. Kurz, D. von der Linde, *Ferroelectrics* **21**, 621 (1978).
- [16] H. Li, F. Zhou, X. Zhang, W. Ji, *Appl. Phys. B* **64**, 659 (1997).
- [17] V. E. Zakharov, A. B. Shabat, *Sov. Phys. JEPT* **36**, 823 (1973).
- [18] Y. Furukawa, K. Kitamura, A. Alexandrovski, R. K. Route, M. M. Fejer, G. Foulon, *Appl. Phys. Lett.* **78**, 1970 (2001).
- [19] E. Fazio, W. Ramadan, A. Petris, M. Chauvet, V. I. Vlad, M. Bertolotti, *Appl. Surf. Sci.* **248**, 97 (2005).
- [20] V. I. Vlad, E. Fazio, M. Bertolotti, A. Bosco, A. Petris, *Appl. Surf. Sci.* **248**, 484 (2005).